Physica C 469 (2009) 188–191

Contents lists available at ScienceDirect

Physica C

journal homepage: www.elsevier.com/locate/physc

Characteristic study of high-T_c superconducting maglev under side-loading

Wei Wang, Jiasu Wang *, Wei Liu, Jun Zheng, Qunxu Lin, Siting Pan, Zigang Deng, Guangtong Ma, Suyu Wang

Applied Superconductivity Laboratory, M/S 152#, Southwest Jiaotong University, Chengdu, Sichuan 610031, PR China

ARTICLE INFO

Article history:
Received 16 January 2009
Accepted 27 January 2009
Available online 3 February 2009

PACS:
84.71.Ba

Keywords:
High temperature superconductor (HTSC)
Maglev vehicle
Resonant frequency (RF)
Pre-load

ABSTRACT

In practical application of High-T_c Superconducting (HTS) maglev, slant is an observable defect. It was caused by constantly one side on and off the vehicle by passengers. So far, this phenomenon has not been reported yet. In order to understand its influence on the stability of the HTS maglev, we experimentally studied the dynamic characteristic and slant effect of HTS maglev under center-load and side-load. It was found that load destabilizes the vehicle, and the side-load can obviously slant the vehicle body. In the end, the pre-load method was proposed to enhance the dynamic stability and suppress the slant, which proved to be considerably effective. These results are critical in practical running of HTS maglev.

1. Introduction

High-T_c superconducting (HTS) levitation [1] has been applied in many fields such as superconducting magnetic bearing (SMB) [2], maglev launch system [3], HTS maglev [4,5], etc. Among them, HTS maglev has been highlighted as a candidate for the next generation's transportation utility with its achievable high-speed [6], high-efficiency, low-noise, environmental-friendly, frictionless and self-stable. However, the passive levitation of high-T_c superconductor (HTSC) leads to a few obstacles, among them, how to enhance the dynamic stability is one of the most important. In an early age, Moon et al. [7] and Chang et al. [8] had found the dynamic stiffness of HTSC is given by the slope of the minor loop. Sugiura [9,10] had numerically studied the free vibration of a HTSC levitated above a permanent magnet (PM). Some methods such as super-cooling [11] and pre-loading [12] were successfully applied to enhance the performance. In our previous work, we studied the dynamic performances of HTS maglev under different field cooling height (FCH) [13] and applies pre-load method to suppress its height-decay [14]. However, the study of HTS maglev under particular loading conditions such as side-loading has not been reported yet.

Since the first man-loading HTS maglev successful operated in 2000, tens of thousands passengers had taken on the vehicle [15]. In practical man-load running, we had found that with a constantly one side boarding, the vehicle slanted observably. This paper dedicates to study the change of performance due to side-loading. Then a pre-load method is proposed to reinforce the performance. The pre-load means, after field cooling (FC), move the vehicle to a height that is lower than the work height for several minutes to trap more flux before operation.

2. Experiment

A simplified HTS maglev is employed in this experiment [13]. Its parameters are 0.8 m in length, 0.6 m in width and 0.35 m in height, weights 45 kg in total (including two vessels and liquid nitrogen). The two liquid nitrogen vessels contain 42 rectangular (64 mm × 32 mm × 12 mm, prepared in ATZ, Germany) melt-textured bulk YBCO averagely arranged at each bottom. The vehicle was cooled at FCH 45 mm, and then freely levitated above the permanent magnetic guideway (PMG). Four accelerometers were fixed at four corners (Fig. 1) on the board to measure its vertical vibration; another two accelerometers were installed above the center of each vessel (Fig. 1) to record the lateral vibration. An impulse force in either vertical or lateral direction was given to the vehicle at some specified points by an impulse hammer. The free vibration curves after the impulse force were collected by the accelerometers and analyzed by analyzer of B&K Company. The sampling time was set to 16 s, and the analysis frequency was set to 1600 Hz. Through twice integrations and FFT analysis, the frequency domain responses and the vibration parameters such as resonant frequency (RF) and damping ratio were obtained.

* Corresponding author. Tel.: +86 28 87601794; fax: +86 28 87603310.
E-mail addresses: frank.weiwang@gmail.com (W. Wang), asclab@asclab.cn (J. Wang).

0921-4534/$ - see front matter © 2009 Elsevier B.V. All rights reserved.
doi:10.1016/j.physc.2009.01.015

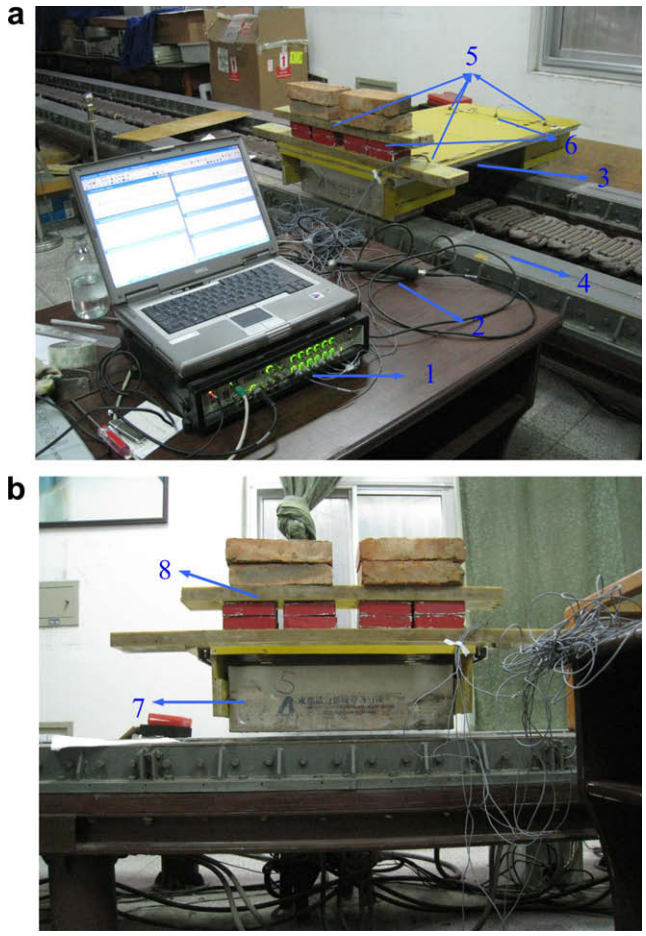

Fig. 1. Experiment set-ups: (1) B&K analyzer; (2) impulse hummer; (3) a simplified HTS maglev; (4) PMG; (5) four vertically installed accelerometers; (6) two laterally installed accelerometers; (7) liquid nitrogen vessel and (8) loads.

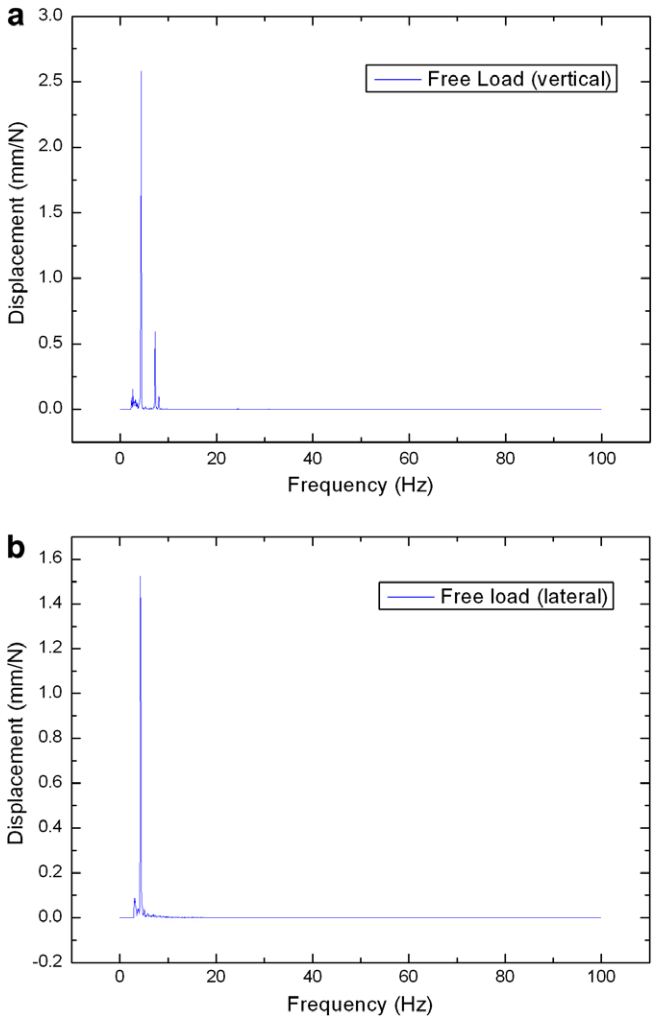

Fig. 2. Frequency domain impulse responses in free-load section: (a) vertical response, the peak value correspond to 4.313 Hz and (b) lateral response, the peak value correspond to 4.250 Hz.

The whole experiments processed in four sections: (1) free-load (without loads); (2) 20 kg center-load or side-load; (3) 40 kg center-load or side-load and (4) pre-load. Here we denote center-load as loads added along the vehicle center along the running direction, side-load as loads added along the side of the vehicle (Fig. 1).

During first three sections, the HTS bulks were cooled at FCH 45 mm for 30 min, and then freely levitated above the PMG for 5 min for flux creeping time [16], measure the vertical and lateral RF (only for Section 1), record the heights of four corners of the vehicle (for Section 2–4). Then add the loads on the board along the line parallel to the tracks (see Fig. 1), measure the RF and heights. Then undo the loads, measure its RF and heights again. In the pre-load section, after cooled at the same FCH, 155 kg loads were center-loaded on board for 10 min, and then relieved to measure its RF and heights, then redo the 40 kg side-load as Section 3.

3. Results and discussion

Fig. 2 is the measured frequency domain response of vertical and lateral vibrations in Section 1, we observed only one RF in both vertical and lateral directions. The vertical and lateral RF are 4.313 Hz and 4.250 Hz respectively, which means the HTS maglev have difficulties to resist low frequency disturbs.

Fig. 3 is the measured RF (as the peak in Fig. 2) change with different load conditions. Both Fig. 3a and b show that when the loads were onboard (during-load in Fig. 3), the RF is smaller than empty load, lead to the destabilization of the vehicle. By increasing the loads (from 20 kg to 40 kg), the RF drops more drastically. Therefore loads are essentially detrimental for the dynamic stability. After taking the load off, the RF bounced back to a similar value as before-load. In Sections 2 and 3, after-load RF increased slightly than before-load. However, in the pre-load section, vertical RF decreased slightly as shown in Fig. 3a.

While comparing side-load with center-load, there is no conspicuous distinctions were found. Side-load doesn't harm more than center-load to the dynamic stability (at least when the loads are not too far away from the vehicle center).

In Section 4 after pre-load, the empty load RF had been notably raised up, and the dynamic stability had been remarkably enhanced. The before-load vertical RF rose 23.3% from 4.313 Hz to 5.625 Hz, while the lateral RF rose 47.1% from 4.25 Hz to 6.25 Hz. And both the during-load and after-load RF were risen up distinctively as shown in Fig. 3.

Fig. 4 is the measured slanting angle of vehicle body due to different load conditions. We can see that the side-load slanted the vehicle body obviously. Even after taking the loads off, a slanting angle still exists (denote as residue angle). In Section 2, while 20 kg was side-loaded, the vehicle slanted 0.33°; after undo the loads, the residue angle was 0.19° (58%). In Section 3, while 40 kg was

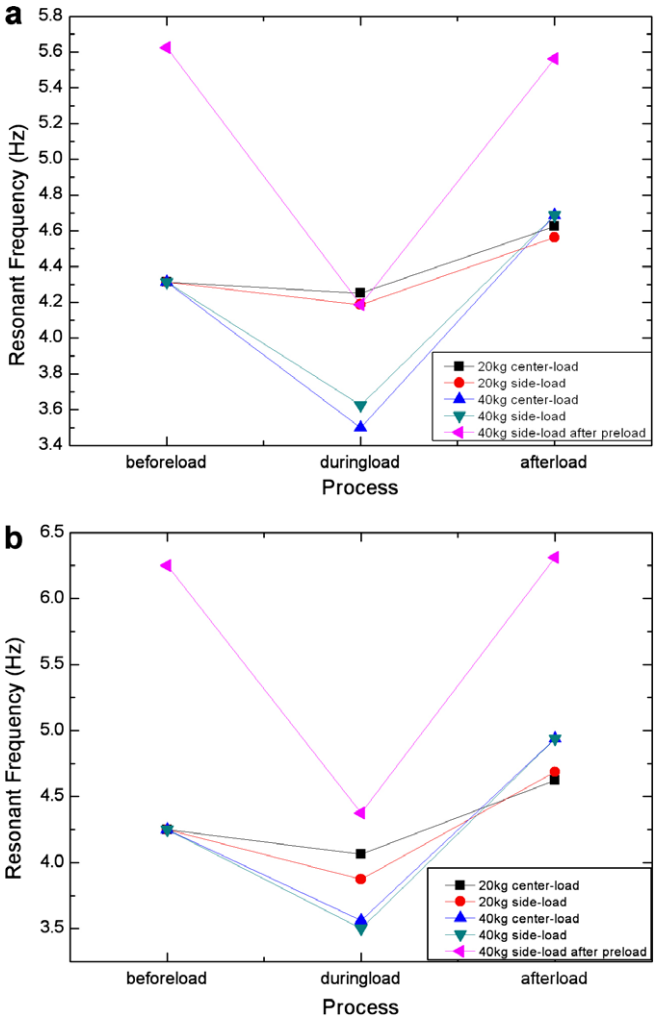

Fig. 3. Resonant frequency changes in three processes with different load conditions. Before-load stands for the condition before loads were added on; during-load stands for when loads were on the vehicle; after-load stands for when loads were taken off: (a) measured vertical RF in different load conditions and (b) measured lateral RF in different load conditions.

side-loaded, the vehicle slanted 0.86°, the residue angle was 0.36° (42%). In Section 4, after pre-loaded, and 40 kg was side-loaded, and the vehicle slanted 0.44° (51% of that in Section 3), the residue angle was greatly suppressed to 0.03° (8% of that in Section 3).

In the following paragraphs, we discuss the slant of vehicle body, change of RF, and the feasibility of pre-load method.

As shown in Fig. 5, side-load can be equalized as a center-load and an additional torque M. Let m' be the mass of the vehicle and g be the gravitational acceleration, thus the left vessel bears a vertical force $F_{\text{left}} = (m'g + F_Z)/2 + M/l_1$, and the right vessel bears a vertical force $F_{\text{right}} = (m'g + F_Z)/2 - M/l_1$. The left and right vessels were bearing different forces, eventually caused the slant of vehicle body as shown in Fig. 4. The levitation forces F_{left} and F_{right} is the vertical component of Eq. (1)

$$F = \int_V \mathbf{J} \times \mathbf{B} dV \tag{1}$$

while the guidance force is the lateral component of above equation. $\boldsymbol{J}$ stands for the induced supercurrents; $\boldsymbol{B}$ is the external magnetic fields.

As shown in Fig. 5, the HTS maglev was considered as a two dimensional dynamic system. Take vertical vibration for example,

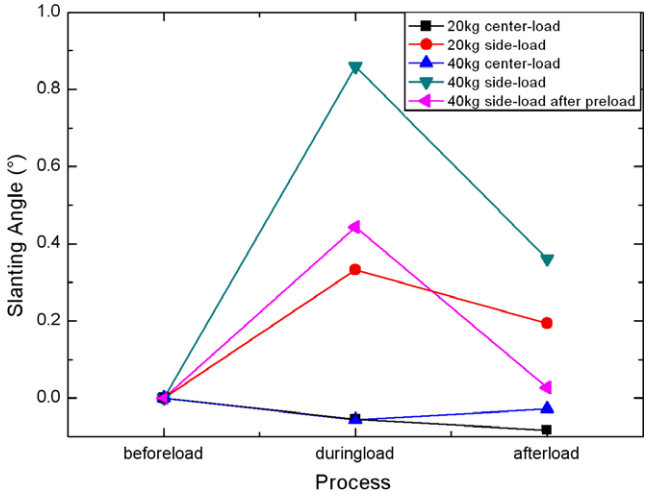

Fig. 4. Slant angle in three processes with different load conditions. The positive value means the vehicle tilting toward the side of the load (Fig. 1).

after a vertical impulse excitation, the vertical free vibration obeys Eq. (2),

$$m\ddot{z} + c_z\dot{z} + k_z z = 0 \tag{2}$$

where z is the vertical coordinate relative to the equilibrium point, m is the levitated mass (equals to m', m' + 20 kg or m' + 40 kg), k_z is the vertical dynamic stiffness equals to $k_{z1} + k_{z2}$, c_z is the vertical damping coefficient equals to $c_{z1} + c_{z2}$. From Eq. (2) we get the vehicle's vertical RF as Eq. (3)

$$f_{\text{n.vertical}} = \sqrt{k_z/m}\Big/2\pi \tag{3}$$

In this experiment as shown in Fig. 5, because $l_2 > l_1/2$, after side-loading, $F_{\text{right}} < m'g/2$, which means the right vessel bore less force and an un-notable ascendance ($1 \sim 2$ mm) was observed. Meanwhile, the left vessel descended drastically (nearly 4.5 mm for 20 kg and 15 mm for 40 kg). Thus we assume k_{z2} and k_{x2} did not change in comparison with k_{z1} and k_{x1}. After side-loading, the left vessel moved downward and induced more supercurrents to provide more connections with the external fields. Thus, the vertical dynamic stiffness k_{z1} increased. Meanwhile, the levitated mass m increased even faster than k_{z1}. Therefore, through Eq. (3), the during-load RF decreased as shown in Fig. 3. After undone the loads, because more supercurrents were induced, thus the dynamic stiffness is still larger than original value, which explains why the after-load RF increased slightly in Fig. 3. At the same time, due to the hysteresis of the left HTSC, a residue angle was produced as in Fig. 4. The lateral dynamic stiffness changes can be explained similarly.

In Section 4, during pre-loading, 155 kg loads were imposed on the board, the bottom of the vessels descended from 34 mm above the PMG to 16.5 mm (17.5 mm downward). After the loads were undone, the vessels restored to 25 mm. The downward movement of vessels induced more supercurrents inside the HTSC, which strengthened the liaisons between the bulks and the PMG, thus the dynamic stiffness increased after pre-load. The increase of dynamic stiffness leads to the increase of RF through Eq. (3). Thus pre-load method is available and practical to enhance the dynamic stability. As for the suppressing of slanting angle, it could be explained similarly. More supercurrents inside the HTSC means more capable to resist external changes, that is why the slant was effectively suppressed after pre-loading.

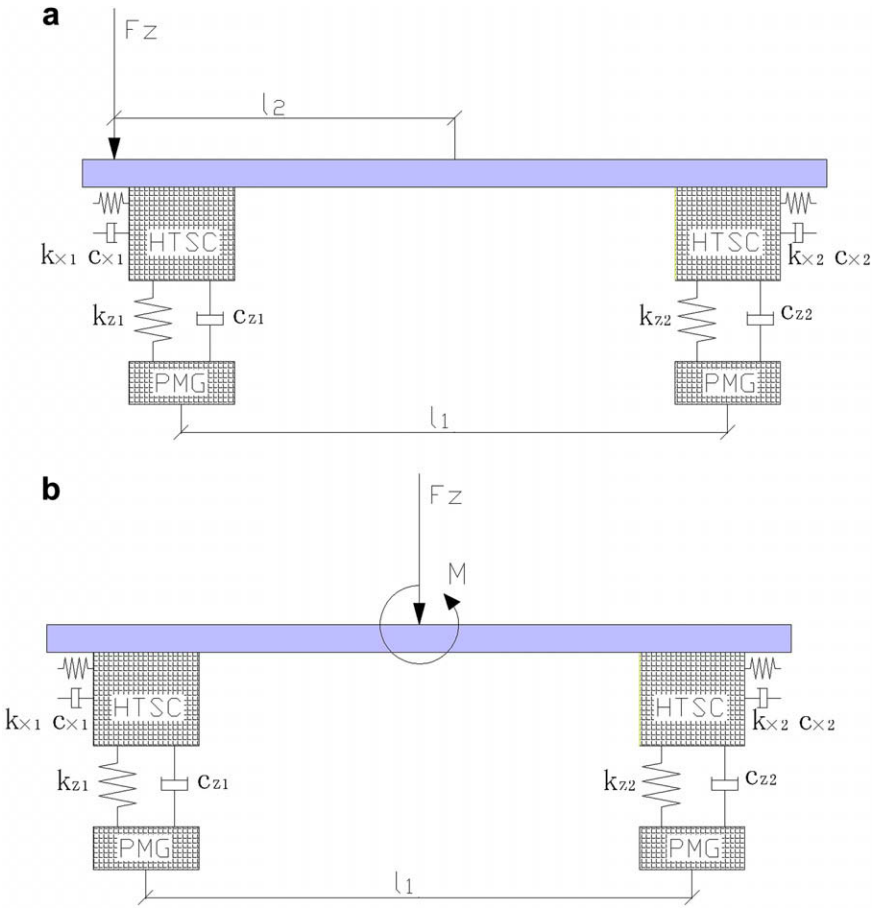

Fig. 5. Illustration of force equalization and the dynamic model of the vehicle: (a) vehicle with side-load; (b) equalization of the side-load, while the torque $M = F_Z \times l_2$. In this experiment, the parameters are: l_1 = 0.85 m, l_2 = 0.5 m, F_Z = 20*g* N or 40*g* N (*g* stands for gravitational acceleration). k_{z1}, k_{z2} stands for the vertical dynamic stiffnesses of the left and right vessel; c_{z1}, c_{z2} stands for the vertical damping coefficients; k_{x1}, k_{x2} stands for the lateral dynamic stiffnesses; c_{x1}, c_{x2} stands for the lateral damping coefficients.

4. Conclusion

The dynamic stability and slant effect of HTS maglev under side-loading was studied, it was found that: (1) loads could drastically decrease the RF, destabilize the HTS maglev; (2) side-load slants the HTS maglev and causes a residue angle; (3) pre-load method is effective in enhancing the dynamic stability and suppressing the slant. These results are critical in optimal design and practical running of HTS maglev.

Acknowledgements

The author would like to thank Ruibin Dong for his assiduous assistance in establishing the platform. This work is supported by the National High Technology Research and Development Program of China (2007AA03Z210), the National Natural Science Foundation in China (50677057).

References

[1] J.R. Hull, Supercond. Sci. Technol. 18 (2000) R1.
[2] M. Strasik et al., IEEE Trans. Appl. Supercond. 17 (2007) 2133.
[3] W.J. Yang, Z. Wen, Y. Duan, X.D. Chen, M. Qiu, Y. Liu, L.Z. Lin, IEEE Trans. Appl. Supercond. 16 (2006) 1108.
[4] J. Wang et al., Physica C 378–381 (2002) 809.
[5] L. Schultz, O. deHaas, P. Verges, C. Beyer, S. Röhlig, H. Olsen, L. Kühn, D. Berger, U. Noteboom, U. Funk, IEEE Trans. Appl. Supercond. 15 (2005) 2301.
[6] J. Wang, S. Wang, C. Deng, Y. Zeng, H. Song, H. Huang, Int. J. Mod. Phys. B 19 (2005) 399.
[7] F.C. Moon, K.C. Weng, P.Z. Chang, J. Appl. Phys. 66 (1989) 5643.
[8] P.Z. Chang, FC. Moon, J.R. Hull, T.M. Mulcahy, J. Appl. Phys. 67 (1990) 4358.
[9] T. Sugiura, H. Fujimori, IEEE Trans. Appl. Supercond. 32 (1996) 1996.
[10] T. Sugiura, M. Tashiro, Y. Uematsu, M. Yoshizawa, IEEE Trans. Appl. Supercond. 7 (1997) 386.
[11] H. Konishi, M. Isono, H. Nasu, M. Hirose, Physica C 392–396 (2003) 713.
[12] N. Koshizuka et al., Physica C 378–381 (2002) 11.
[13] Z. Deng, J. Zheng, H. Song, L. Liu, L. Wang, Y. Zhang, S. Wang, J. Wang, IEEE Trans. Appl. Supercond. 17 (2007) 2071.
[14] Z.G. Deng, J. Zheng, J. Zhang, J.S. Wang, S.Y. Wang, Y. Zhang, L. Liu, Physica C 463–465 (2007) 1293.
[15] J.S. Wang, S.Y. Wang, Y.W. Zeng, C.Y. Deng, Z.Y. Ren, X.R. Wang, H.H. Song, X.Z. Wang, J. Zheng, Y. Zhao, Supercond. Sci. Technol. 18 (2005) S215.
[16] Y.S. Tseng, C.H. Chiang, W.C. Chan, Physica C 411 (2004) 32.